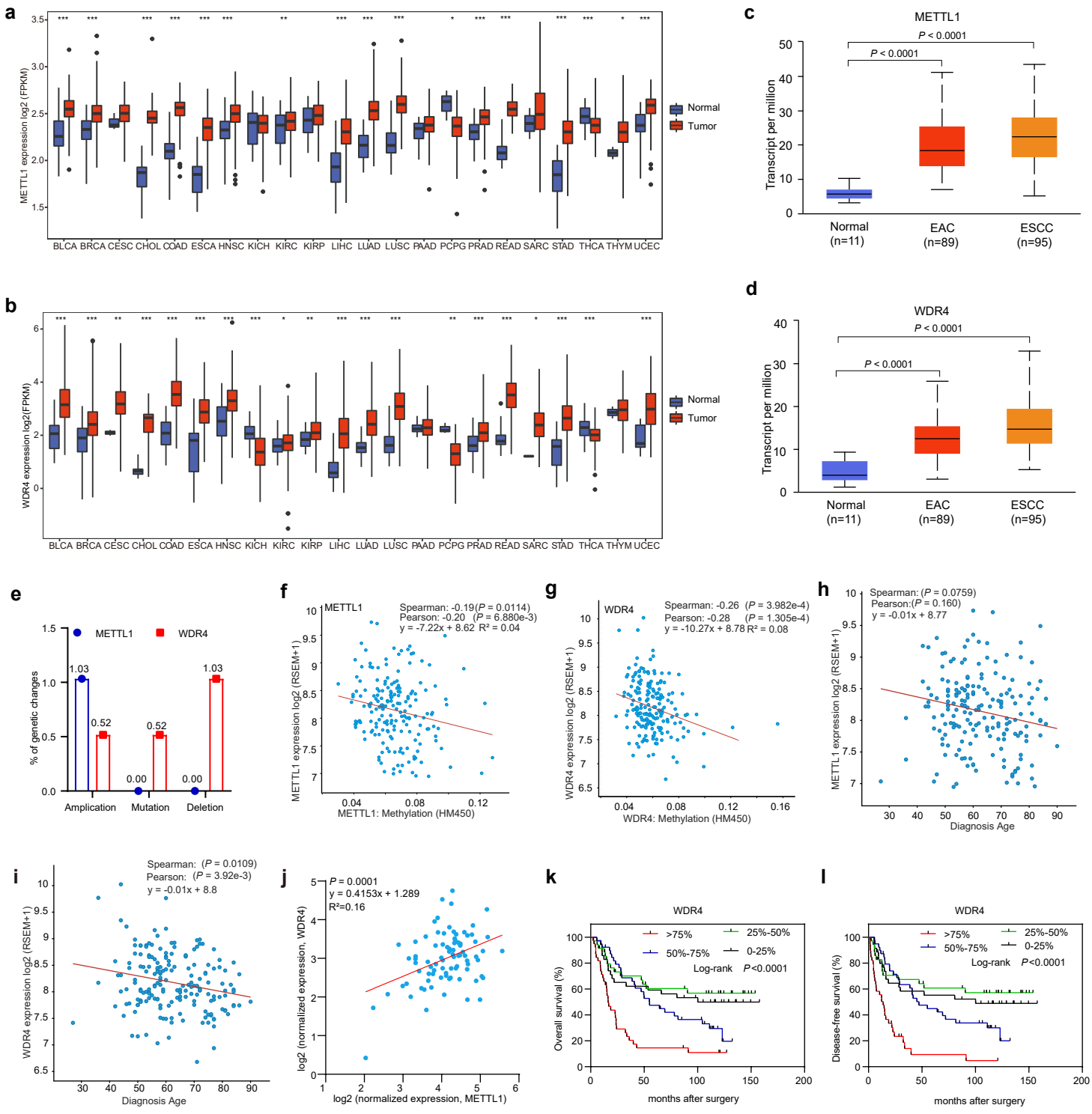

Supplementary Figure 1 Clinical association of METTL1 and WDR4 in ESCCs.
a-**b**, The relative mRNA levels of METTL1 (**a**) and WDR4 (**b**) in 22 cancer types in TCGA. *P < 0.05, **P < 0.01, ***P < 0.001.The exact P values and sample size for normal and tumor tissues were provided in a source data file. **c**-**d**, Quantification of METTL1 (**c**) and WDR4 (**d**) expression in normal esophageal tissues and esophageal tumors. **e**, Gene amplification, mutation, and depletion of METTL1 and WDR4 in ESCCs. **f**-**g**, Correlation between the mRNA expression and DNA methylation of METTL1 (**f**) and WDR4 (**g**) in ESCC. **h**-**i**, The correlation between patient age and METTL1 (**h**) or WDR4 (**i**) expression level. **j**, Correlation between the expression of METTL1 and WDR4 in ESCCs. **k**-**l**, Kaplan-Meier analysis of the overall survival (**k**) or disease-free survival (**l**) of ESCC patients based on different H-scores of WDR4. The box plots showing minima, maxima, centre, bounds of box and whiskers and percentile for (**a**-**d**). Data presented as mean ± SD. P values were calculated by two-tailed Mann-Whitney U test for (**a**-**d**), Pearson correlation analysis for (**f**-**i**) and log-rank test for (**k**-**l**). The data underlying **a**-**j** referenced during the study are available in a public repository from the TCGA website (https://www.cancer.gov/about-nci/organization/ccg/research/structural-genomics/tcga). The source data of k and l are protected and are not available due to data privacy laws.

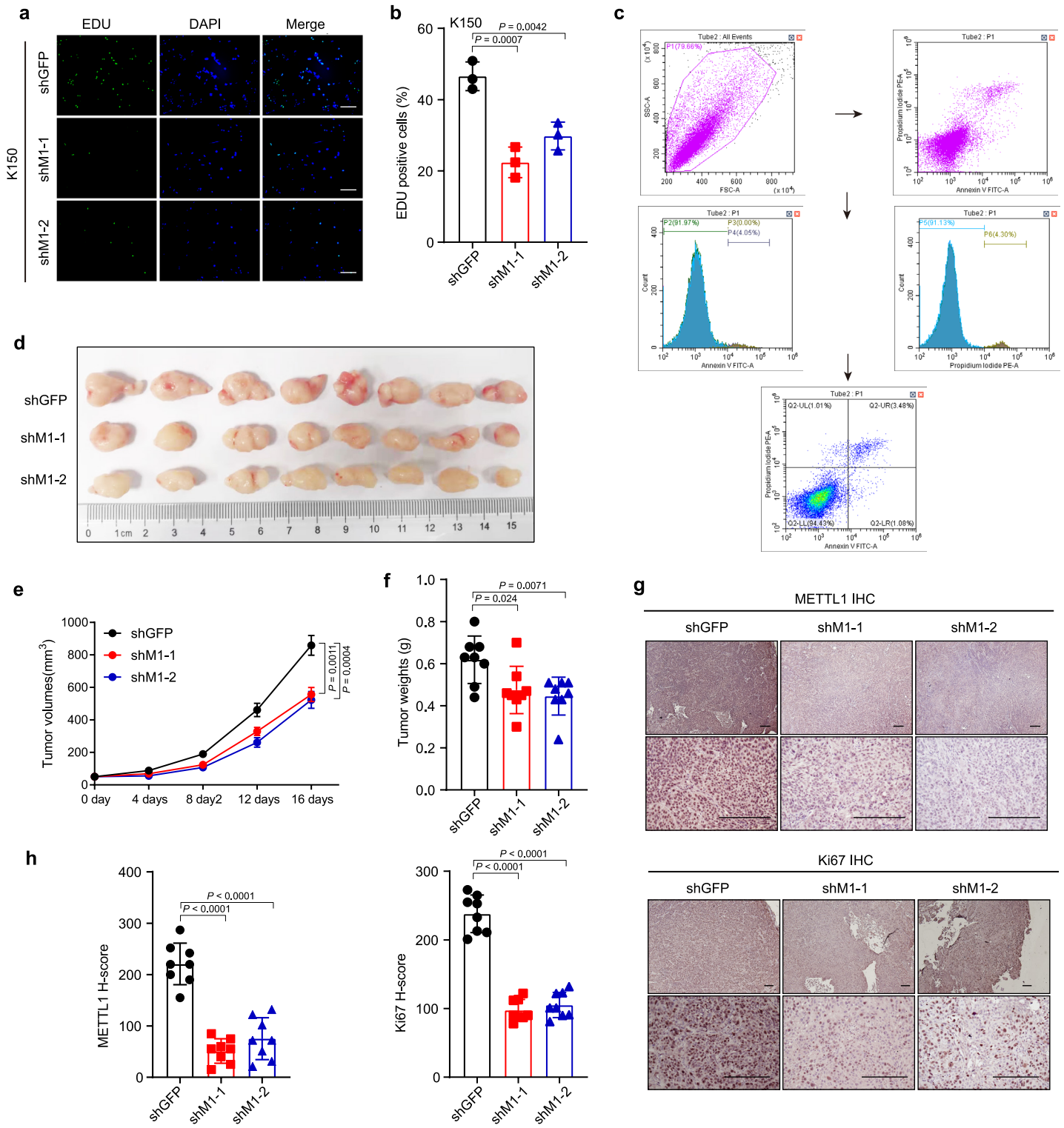

Supplementary Figure 2 METTL1 knockdown impairs ESCC progression in vitro and in xenograft model.
a-b, Edu assay (**a**) and the quantitative analysis (**b**) of METTL1 knockdown and control K150 ESCC cells. Scale bar, 200 μm. **c**, Example of the gating strategy used in the apoptosis assay. **d**, Overview of tumors in xenograft mice model subcutaneously implanted with METTL1 knockdown and control K30 ESCC cells. **e**, Growth curves of tumor volumes in METTL1 knockdown and control K30 ESCC cells. **f**, Tumor weights in METTL1 knockdown and control K30 ESCC cells. **g-h**, Representative images of METTL1 and Ki67 IHC staining (**g**) and the quantitative H-scores (**h**) of tumors obtained from the K150 xenograft model. Scale bar, 200 μm. Data represented as mean ± SD by one-way ANOVA with Dunnett's multiple comparison test from three independent experiments for (**b**) and eight biological independent samples for (**d-g**). Source data are provided as a Source Data file.

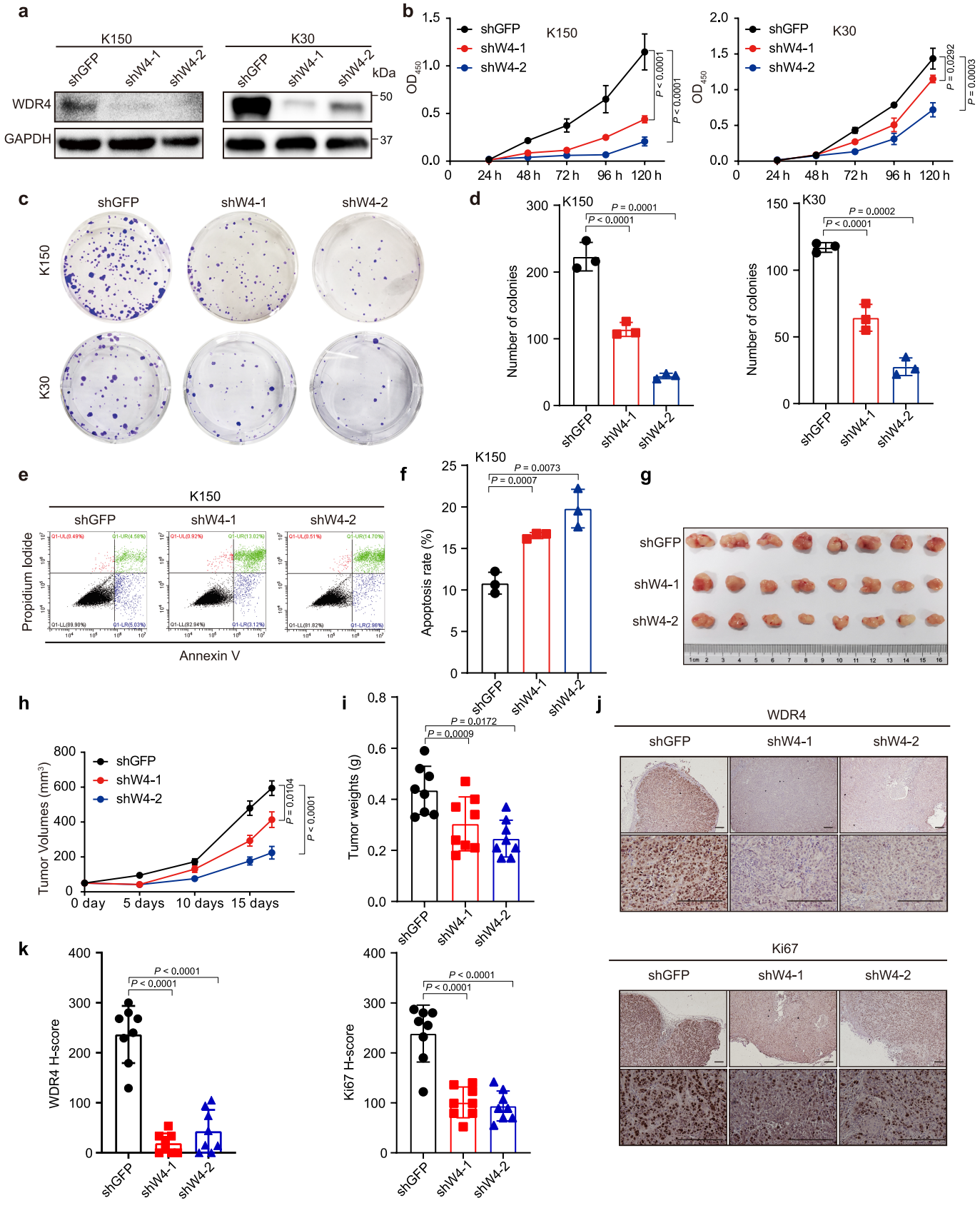

Supplementary Figure 3 WDR4 knockdown impairs ESCC progression in vitro and in vivo.
a, Western blot with indicated antibodies in WDR4 knockdown and control ESCC cells. **b**, CCK8 analysis of WDR4 knockdown and control ESCC cells. **c-d**, Colony-formation assay (**c**) and the quantification analysis (**d**) of WDR4 knockdown and control ESCC cells. **e-f**, Apoptosis assay (**e**) and the quantification analysis (**f**) of WDR4 knockdown and control ESCC cells. **g**, Overview of tumors in xenograft model subcutaneously implanted with of WDR4 knockdown and control K150 ESCC cells. **h**, Growth curves in xenograft model injected with WDR4 knockdown and control K150 ESCC cells. **i**, Tumor weights in xenograft model injected with WDR4 knockdown and control K150 ESCC cells. **j-k**, Representative images of WDR4 and Ki67 IHC staining (**j**) and the quantitative H-scores (**k**) of tumors obtained from the xenograft mice model. Scale bar, 200 μm. Data represented as mean ± SD by one-way ANOVA with Dunnett's multiple comparison test from three independent experiments for (**b**, **d**, and **f**) and eight biological samples for (**h-k**). Source data are provided as a Source Data file.

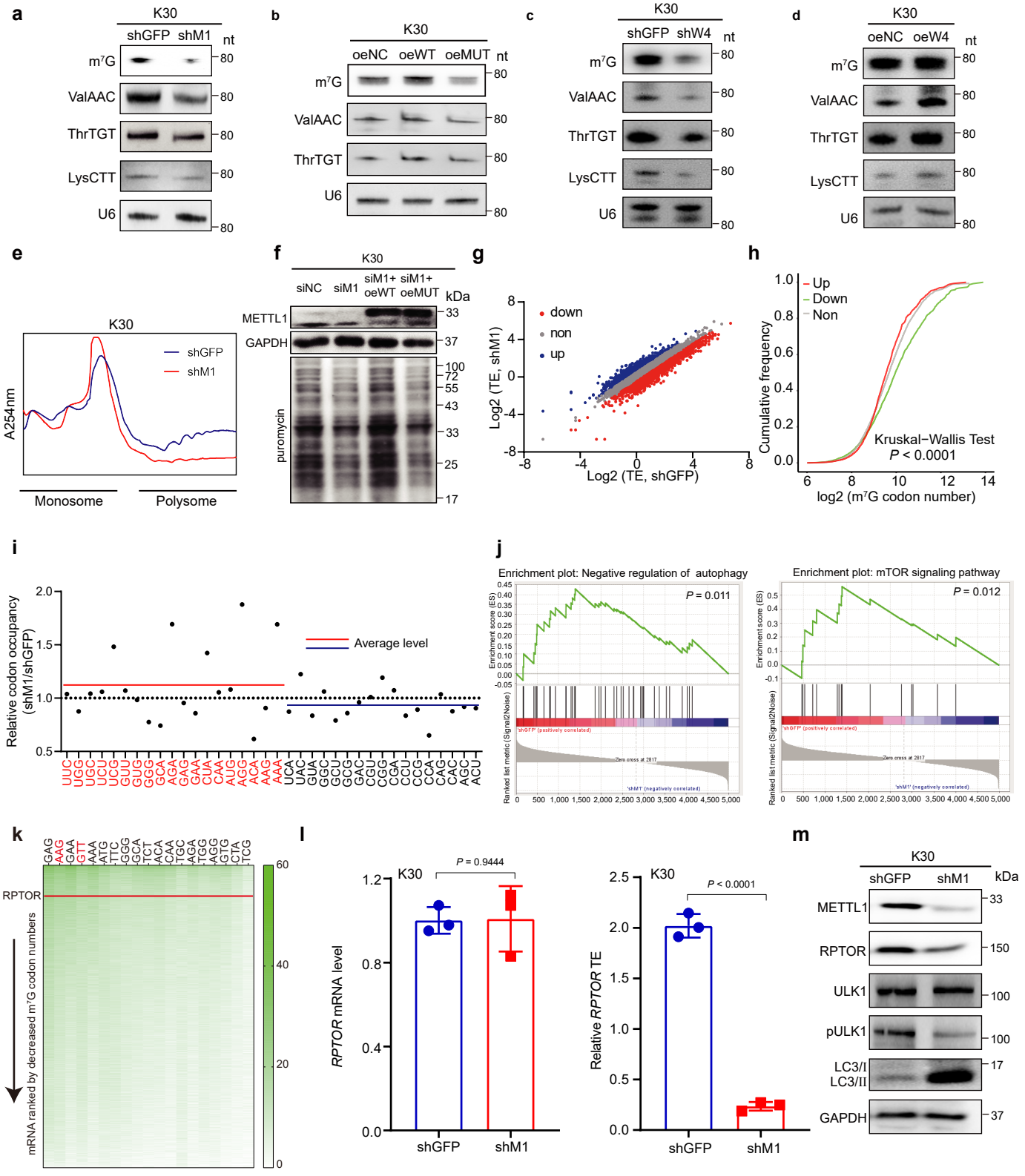

Supplementary Figure 4 METTL1 regulates m^{7}G tRNA modification, tRNA expression and oncogenic mRNA translation.
a-d, Northern blot with indicated tRNA probes in METTL1 depleted K30 cells (**a**), wild type METTL1 or mutant METTL1 overexpressed K30 cells (**b**), WDR4-depleted K30 cells (**c**) and WDR4 overexpressed K30 cells (**d**). U6 snRNA was used as a loading control. **e**, Polysome profiling of METTL1 depleted and control K30 cells. **f**, Puromycin intake assay of METTL1 depleted K30 cells rescued with wild type or catalytic inactive METTL1. **g**, Scatterplot of TEs in the METTL1 knockdown and control cells in the Ribo-seq data. **h**, Codon number in the coding sequence (CDS) region of the genes with increased TEs (up), decreased TEs (down), and other genes (non) in Ribo-seq data in the METTL1 knockdown cells. **i**, Relative ribosome occupancy at individual codons at A sites in METTL1 depleted cells and control cells. Only codons with detectable corresponding tRNA expression were shown. The codons decoded by non-m^{7}G tRNAs (black) and codons decoded by m^{7}G tRNAs (red) were presented. **j**, GSEA analysis of decreased translated mRNAs in Ribo-seq data. **k**, Heatmap showed the enrichment of m^{7}G-related codons in all detected mRNAs. **l**, qRT-PCR analysis of polyribosome-mRNAs and input mRNAs in K30 cells from three independent experiments. **m**, Western blot analysis with indicated antibodies in K30 cells. Data represented as mean ± SD. *P* values are calculated by permutation test for (**j**) and two-tailed unpaired Student's t test for (**i**). Source data are provided as a Source Data file.

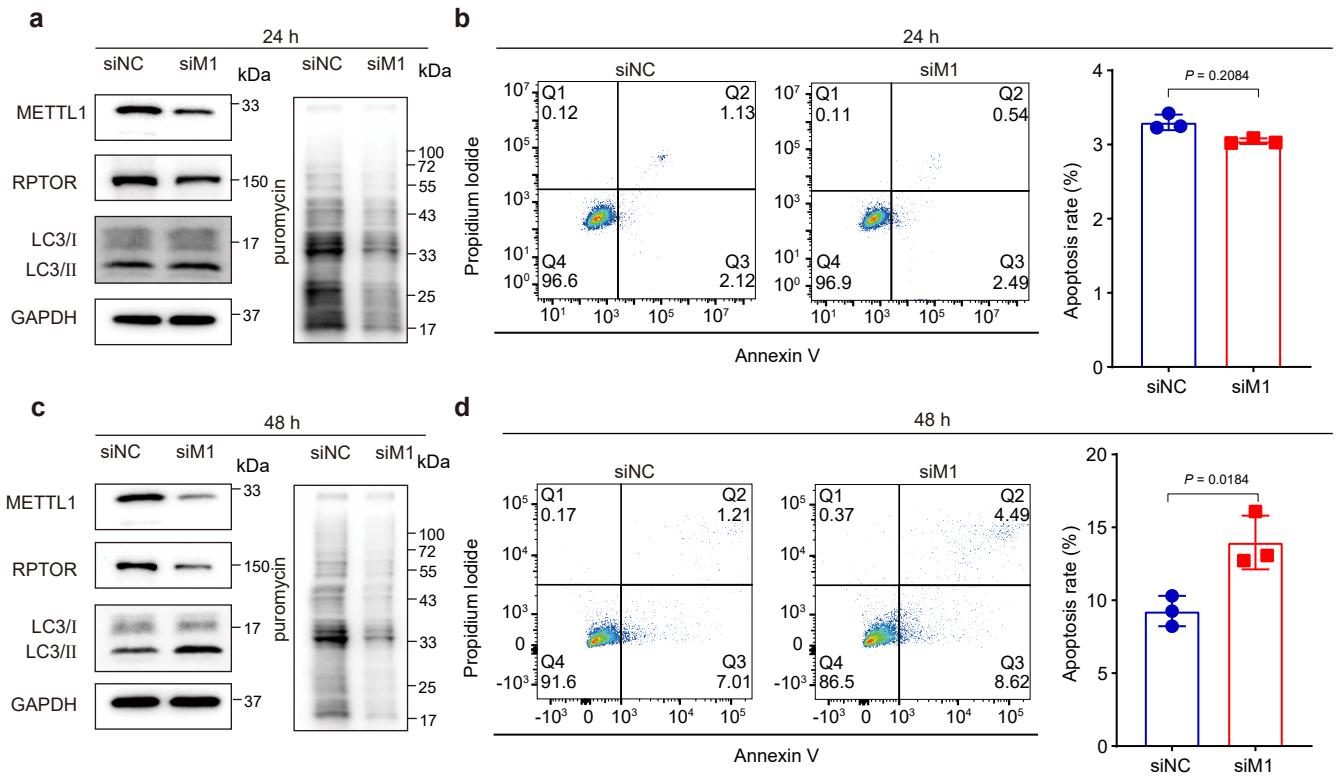

Supplementary Figure 5 Decreased mRNA translation upon METTL1 knockdown leads to impaired cell survival.
a, The puromycin incorporation and protein levels of RPTOR and LC3 at 24 h after METTL1 knockdown in K150 cells. **b**, The apoptosis rate of K150 ESCC cells at 24 h after METTL1 knockdown. **c**, The puromycin incorporation and protein levels of RPTOR and LC3 at 48 h after METTL1 knockdown in K150 cells. **d**, The apoptosis rate of K150 ESCC cells at 48 h after METTL1 knockdown. Data represented as mean ± SD by two-tailed unpaired Student's t test from three independent experiments for (**b** and **d**). Source data are provided as a Source Data file.

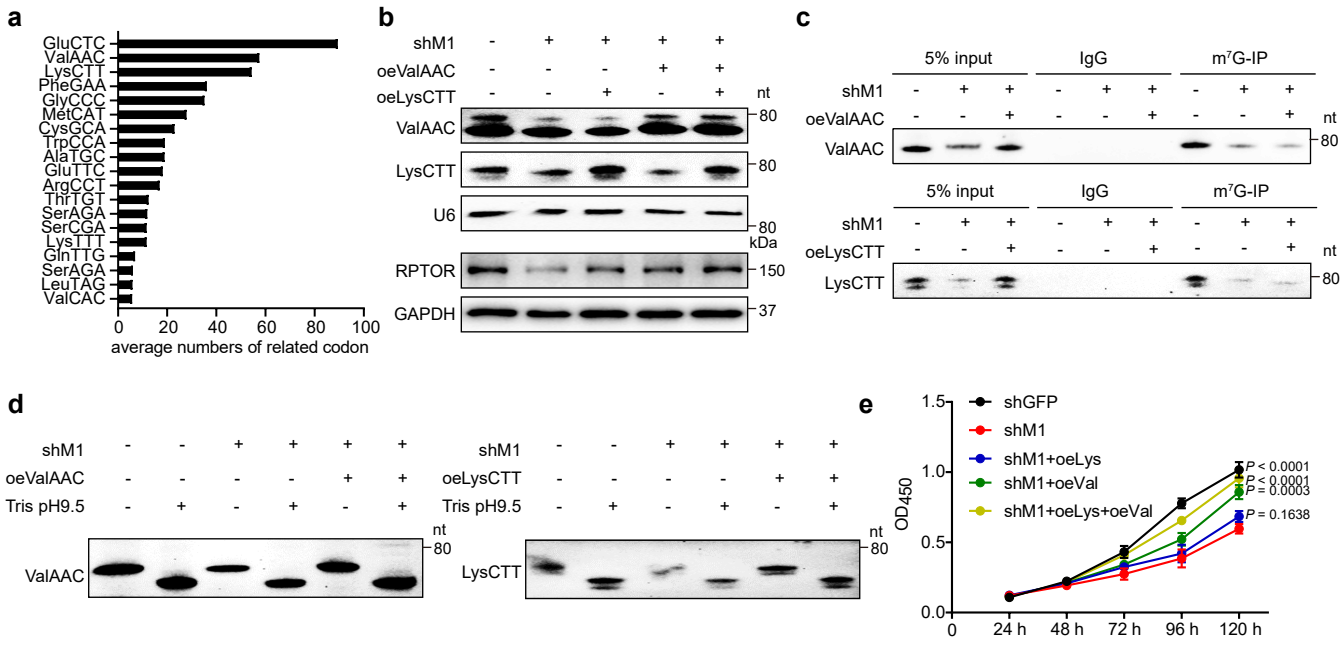

Supplementary Figure 6 m^{7}G-modified tRNAs mediate METTL1's function in ESCC progression.
a, Average number of individual m^{7}G-modified tRNA decoded codons in TE-down mRNAs in K150 ESCC cells. **b**, Northern blot and western blot with indicated probes and antibodies in K150 ESCC cells. **c**, m^{7}G MeRIP-northern blot with indicated probes. **d**, tRNA charging assay to detect the charging of ectopically overexpressed ValAAC and LysCTT tRNAs. **e**, CCK8 assay of METTL1 knockdown K150 ESCC cells with or without tRNA overexpression. Data represented as mean ± SD from three independent experiments for (**e**). Significant difference from shM1 group calculated by one-way ANOVA with Dunnett's multiple comparison test are shown on graphs (**e**). Source data are provided as a Source Data file.

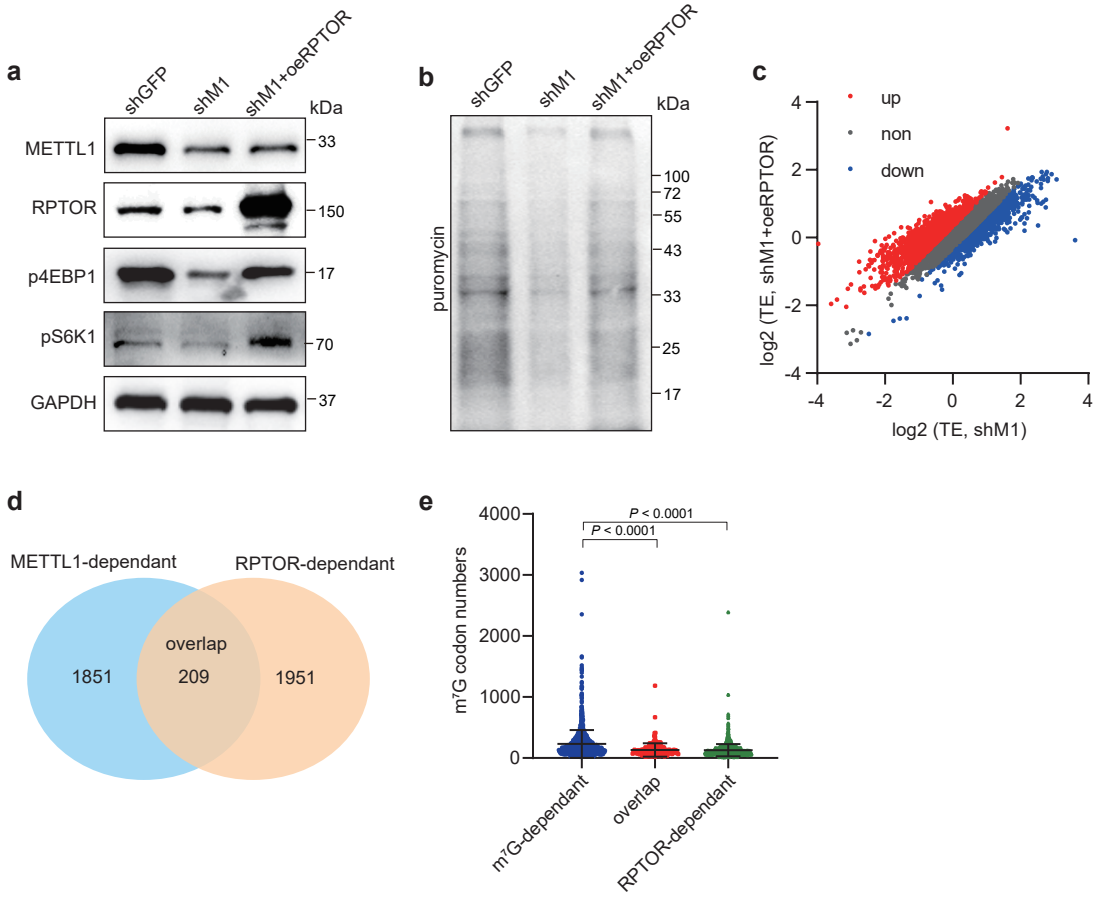

Supplementary Figure 7 Overexpression of RPTOR restores translation of METTL1 depleted ESCC cells.
a, Western blot with indicated antibodies in METTL1 depleted K150 ESCC cells with or without RPTOR overexpression. **b**, Puromycin incorporation assay in METTL1 depleted K150 ESCC cells with or without RPTOR overexpression. **c**, Scatterplot of TEs in the METTL1 knockdown cells with or without RPTOR overexpression. **d**, Overlap of TE down mRNAs upon METTL1 knockdown and TE up mRNAs upon RPTOR overexpression. **e**, Comparison of m^{7}G related codon numbers in METTL1-dependent, RPTOR-dependent and the overlap group. Data represented as mean ± SD by two-tailed Mann-Whitney U test from three biological independent samples. Source data are provided as a Source Data file.

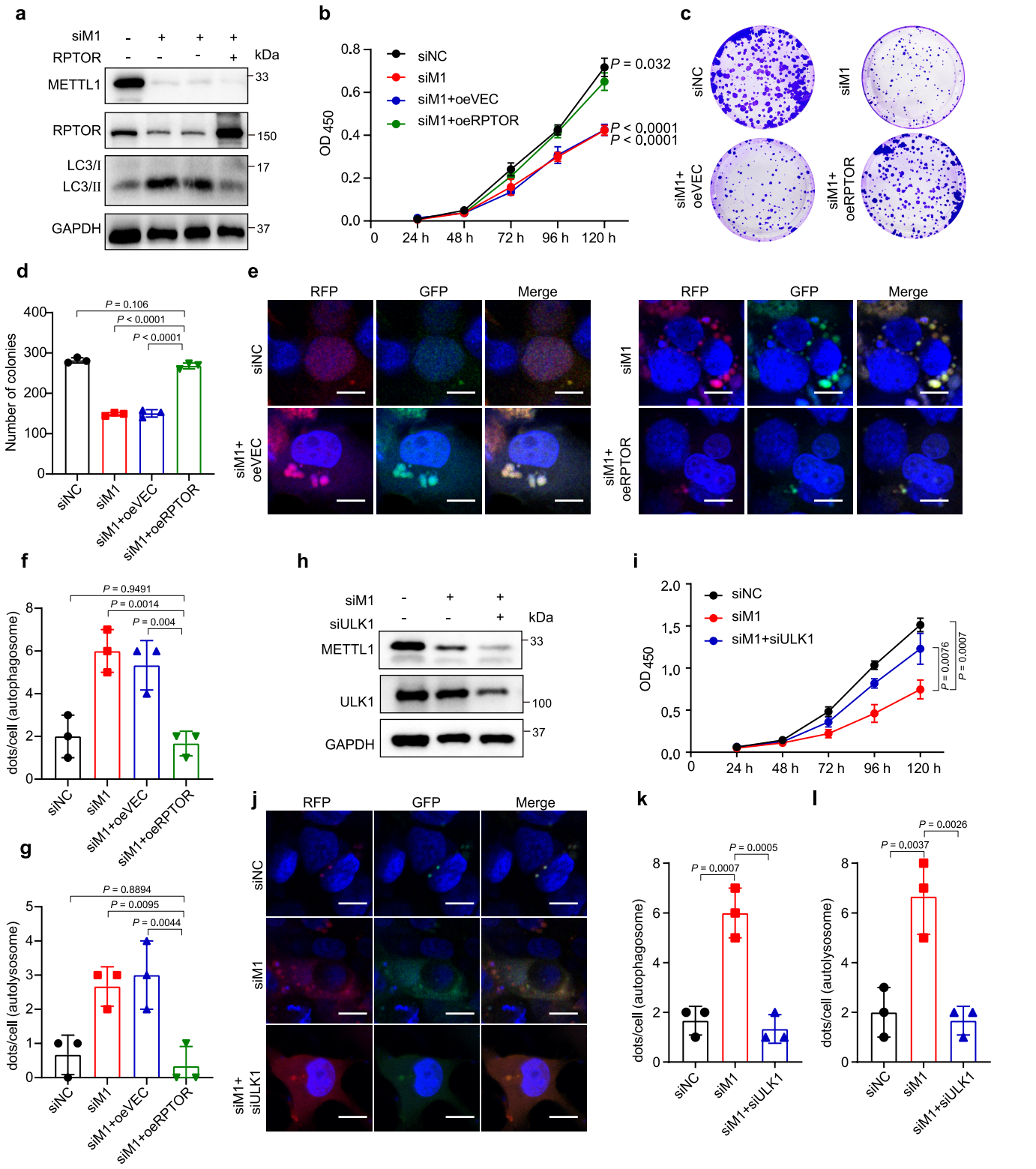

Supplementary Figure 8 RPTOR and ULK1-mediated autophagy play essential roles in ESCC progression in K30 cells.
a, Western blot analysis with indicated antibodies in METTL1 knockdown K30 cells with or without RPTOR overexpression. **b**, CCK8 assay of METTL1 knockdown K30 cells with or without RPTOR overexpression. **c-d**, Colony-formation assay (**c**) and the quantification analysis (**d**) of METTL1 knockdown K30 cells with or without RPTOR overexpression. **e-g**, The autophagic fluxes (**e**) and the quantification analysis (**f**, **g**) of K30 cells stably expressed mRFP-EGFP-LC3 fusion protein. Scale bar, 10 μm. **h**, Western blot analysis with indicated antibodies in K30 cells. **i**, CCK8 assay of METTL1 knockdown K30 cells with or without ULK1 knockdown. **j-l**, The autophagic fluxes (**j**) and the quantification analysis (**k**, **l**) of K30 cells stably expressed mRFP-EGFP-LC3 fusion protein. Scale bar, 10 μm. Data represented as mean ± SD from three independent experiments. Significant difference from siM1+oeRPTOR group calculated by one-way ANOVA with Dunnett's multiple comparison test are shown on graphs (**b**, **d**, **f**, and **g**), and significant difference from siM1+siULK1 group calculated by one-way ANOVA with Dunnett's multiple comparison test are shown on graphs (**i**, **k**, and **l**). Source data are provided as a Source Data file.

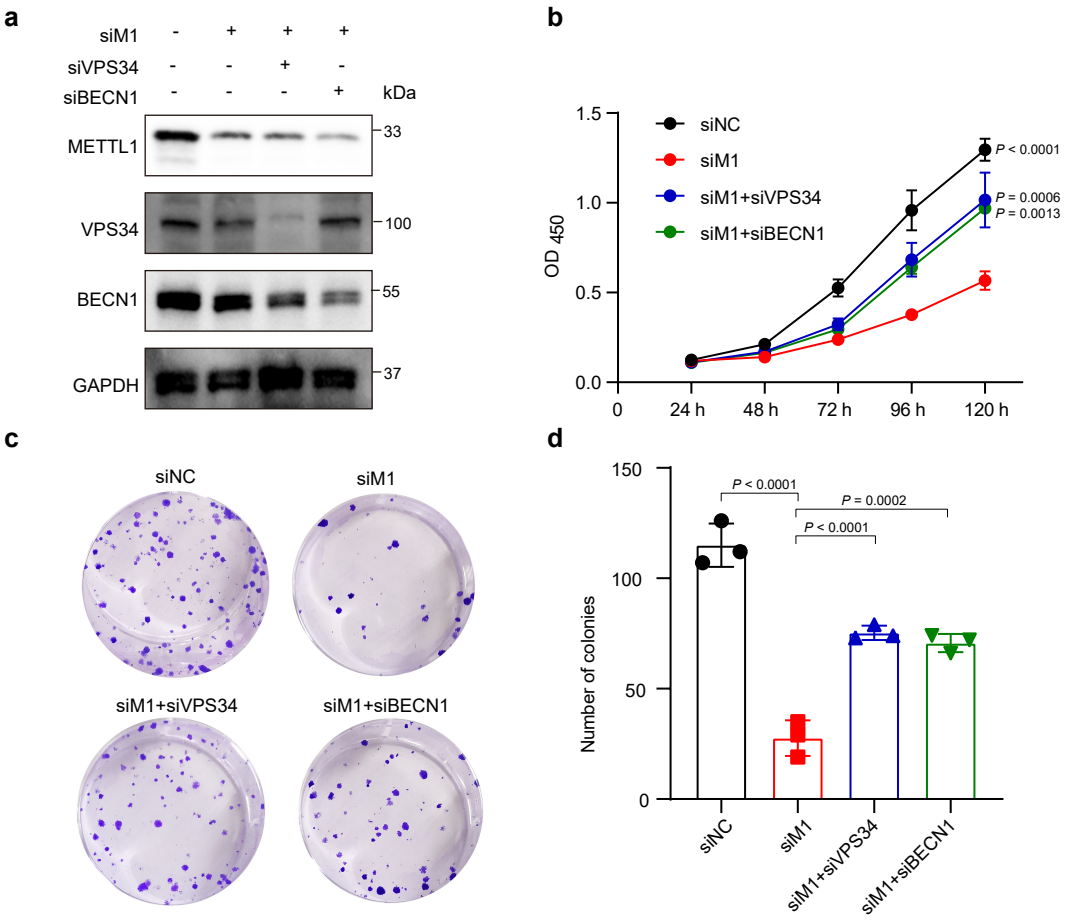

Supplementary Figure 9 VPS34 and BECN1 mediate METTL1's function in ESCC.
a, Western blot analysis with indicated antibodies. **b**, CCK8 assay of METTL1 knockdown K150 cells with VPS34 or BECN1 knockdown. **c**-**d**, Colony-formation assay (**c**) and the quantitative analysis (**d**) of METTL1 knockdown K150 cells with VPS34 or BECN1 knockdown. Data represented as mean ± SD from three independent experiments. Significant difference from siM1 group calculated by one-way ANOVA with Dunnett's multiple comparison test are shown on graphs. Source data are provided as a Source Data file.

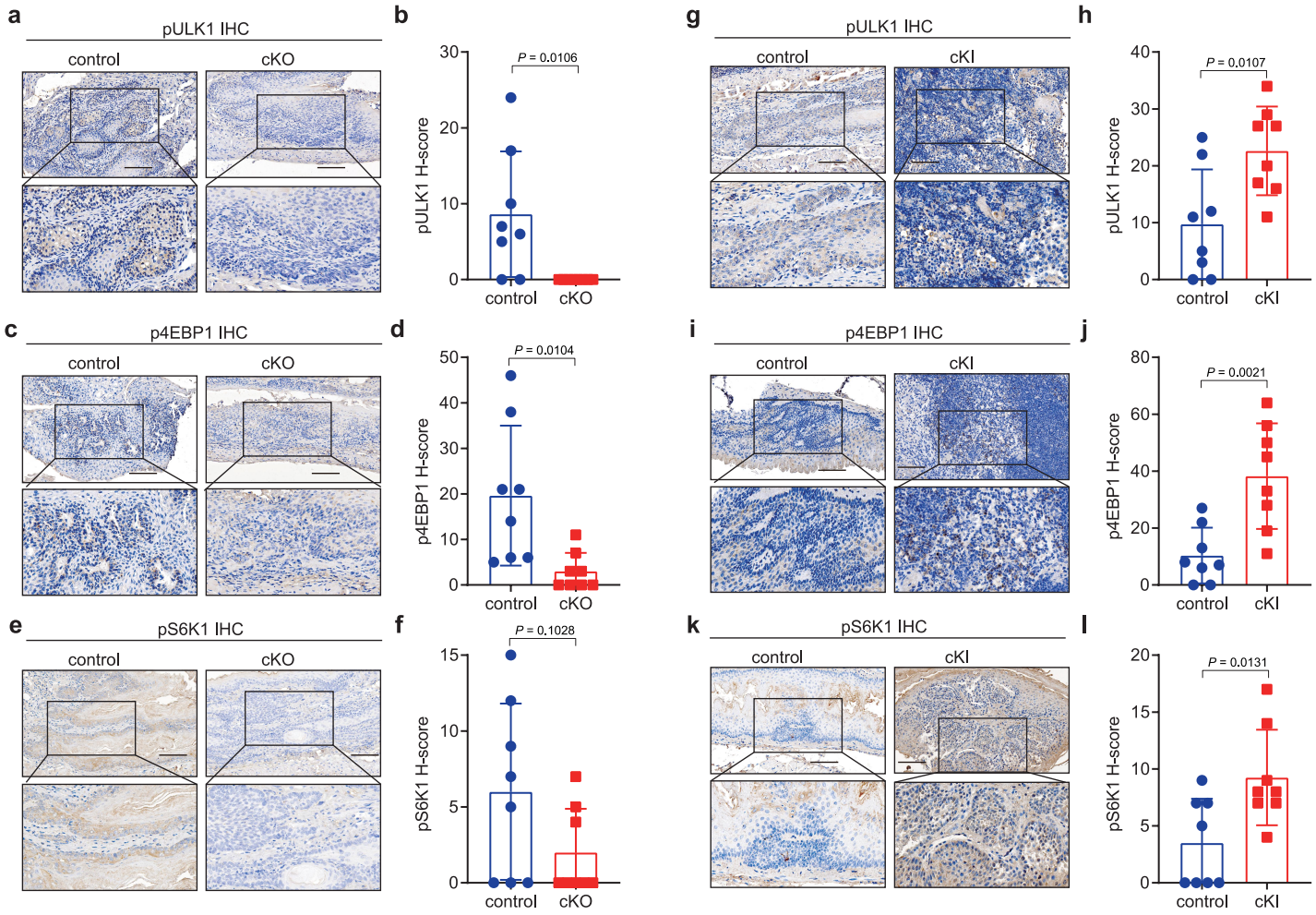

Supplementary Figure 10 The downstream targets of RPTOR were regulated by METTL1 in vivo.
a-b, Representative images (**a**) and the quantification (**b**) of pULK1 IHC staining in *Mettl1* cKO and control mice. Scale bar, 100 μm. **c-d**, Representative images (**c**) and the quantification (**d**) of p4EBP1 IHC staining in *Mettl1* cKO and control mice. Scale bar, 100 μm. **e-f**, Representative images (**e**) and the quantification (**f**) of pS6K1 IHC staining in *Mettl1* cKO and control mice. Scale bar, 100 μm. **g-h**, Representative images (**g**) and the quantification (**h**) of pULK1 IHC staining in *Mettl1* cKI and control mice. Scale bar, 100 μm. **i-j**, Representative images (**i**) and the quantification (**j**) of p4EBP1 IHC staining in *Mettl1* cKI and control mice. Scale bar, 100 μm. **k-l**, Representative images (**k**) and the quantification (**l**) of pS6K1 IHC staining in *Mettl1* cKI and control mice. Scale bar, 100 μm. Data represented as mean ± SD by two-tailed unpaired Student's t test.from eight biological independent samples for each group. Source data are provided as a Source Data file.

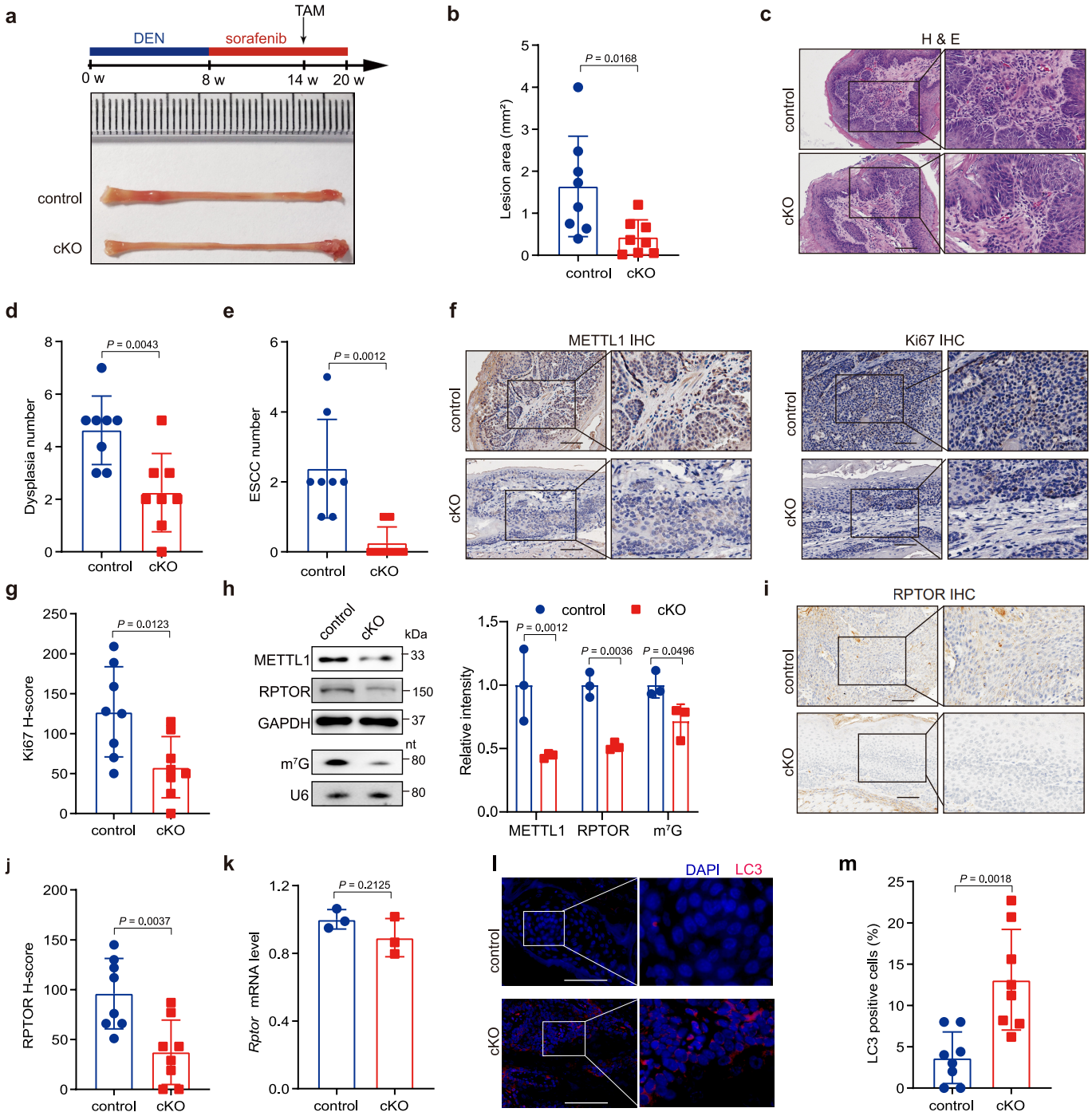

Supplementary Figure 11 Knockout of *Mettl1* inhibits in vivo ESCC progression.
a, Experimental design for ESCC progression model and the representative images of esophageal lesions in *Mettl1* cKO and control mice. **b**, Quantification of lesion areas. **c**, Representative H&E staining of esophagus. Scale bar, 100 μm. **d**, Quantification of dysplasia numbers. e, Quantification of ESCC numbers. **f-g**, Representative images of METTL1 and Ki67 IHC staining (**f**) and the quantification Ki67 H-scores (**g**) in *Mettl1* cKO and control mice. Scale bar, 100 μm. **h**, western blot analysis and northwestern blot analysis showed the m⁷G modification level and indicated protein levels, right panel: quantification of the blot signals. **i-j**, Representative images (**i**) and the quantification (**j**) of RPTOR IHC staining. Scale bar, 100 μm. **k**, qRT-PCR analysis of *Rptor* mRNA level in the cKO and control mice. **l-m**, IF assay (**l**) and the quantification (**m**) of LC3 level. Scale bar, 100 μm. Data represented as mean ± SD by two-tailed unpaired Student's t test from eight biological independent samples for each group for (**a-g**, **i**, **j**, **l**, and **m**) and three biological independent samples for (**h** and **k**). Source data are provided as a Source Data file.

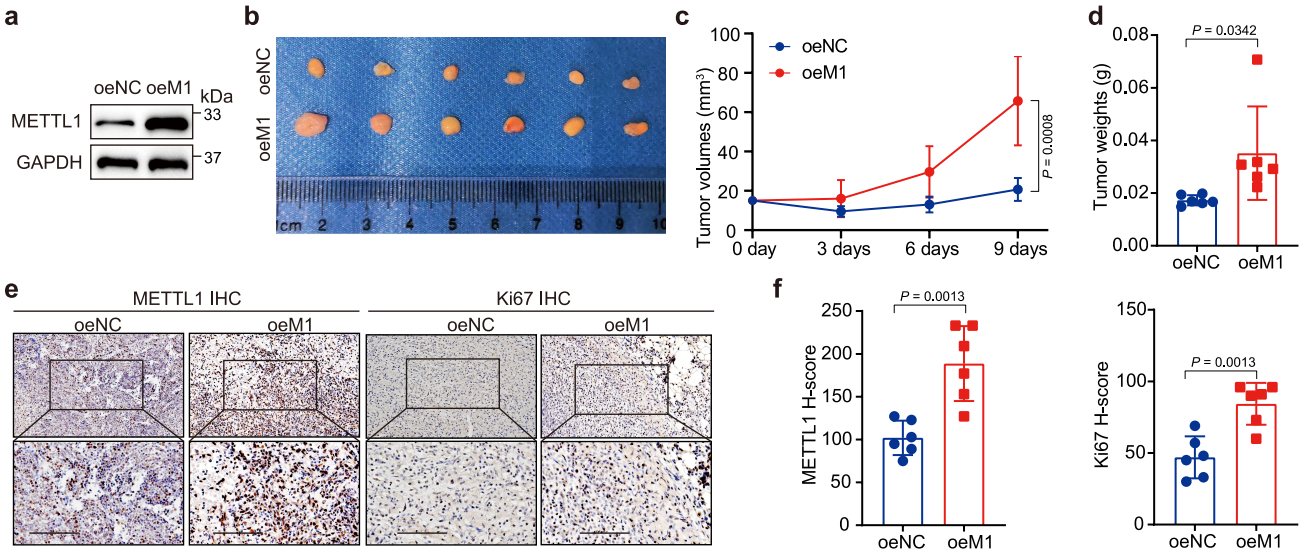

Supplementary Figure 12 METTL1 overexpression promotes ESCC tumorigenesis in xenograft mouse model.
a, Western blot assay showed the indicated protein levels in K150 ESCC cells. **b**, Overview of tumors in xenograft mice model subcutaneously implanted with METTL1 overexpression and control ESCC cells. **c**, Growth curves of tumor volumes in METTL1 overexpression and control group. **d**, Tumor weights in METTL1 overexpression and control group. **e-f**, Representative images of METTL1 and Ki67 IHC staining (**e**) and the quantitative H-scores (**f**) of tumors obtained from the xenograft model. Scale bar, 200 μm. Data represented as mean ± SD by two-tailed unpaired Student's t test from six biological independent samples for each group. Source data are provided as a Source Data file.

Supplementary Table 1. Genes enriched in autophagy and mTOR signaling pathway

Genes enriched in autophagy pathway
SRC
SREBF1
WDR81
DAPK3
ATG2A
ITGB4
QSOX1
BOK
RPTOR
WDR24
TMEM150A
CHMP6
KAT5
CAPN1
UBXN6
KLHL22
EEF1A2
ULK3
ATP6V0D1
MAP1S
CTSD
GPSM1
Genes enriched in mTOR signaling pathway
SREBF1
RPTOR
SFN
PML
POLDIP3
PRR5
EEF2

Supplementary Table 2. Baseline information of 120 patients with esophageal cancer.

Characteristic	Number
Gender	
Female	33 (27.5%)
Male	87 (72.5%)
Age	
Median (range)	58 (38-80)
T category	
T1	2 (1.7%)
T2	30 (25%)
T3	88 (73.3%)
T4	0 (0%)
N category	
N0	67 (55.8%)
N1	51 (42.5%)
N2	2 (1.7%)
Overall stage	
I	3 (2.5%)
II	73 (60.8%)
III	44 (36.7%)
IV	0 (0%)

Supplementary Table 3. Antibodies used in this study.

Antibodies	source	identifier
Rabbit monoclonal anti-WDR4	Abcam	Cat# ab169526
Rabbit polyclonal anti-Ki67	Abcam	Cat# ab15580
Rabbit polyclonal anti-Phospho-ULK1 (ser758)	Affinity	Cat# AF4387
Rabbit polyclonal anti-ULK1	Beyotime	Cat# AF8307
Phospho-4E-BP1 (Thr37/46) (236B4) Rabbit mAb	Cell signaling technology	Cat# 2855
Phospho-p70 S6 Kinase (Thr421/Ser424) Antibody	Cell signaling technology	Cat# 9204
Anti-rabbit IgG HRP-linked Antibody	Cell signaling technology	Cat# 7074S
Anti-mouse IgG HRP-linked Antibody	Cell signaling technology	Cat# 7076S
Rabbit polyclonal anti-LC3	Cell signaling technology	Cat# 2775S
Mouse monoclonal 7-methylguanosine (m^7G) antibody	MBL International	Cat# RN017M
Mouse monoclonal anti-puromycin	Millipore	Cat# MABE343
PI3 Kinase p110 Alpha Monoclonal antibody	Proteintech	Cat# 67071-1-Ig
Rabbit polyclonal anti-METTL1	Proteintech	Cat# 14994-1-AP
Mouse monoclonal anti-RPTOR	Proteintech	Cat# 20984-1-AP
Rabbit polyclonal anti-GAPDH	Proteintech	Cat# 10494-1-AP
Rabbit polyclonal anti-VPS34	Proteintech	Cat# 12452-1-AP
Rabbit polyclonal anti-BECN1	Proteintech	Cat# 11306-1-AP
Goat anti-rabbit IgG H&L DyLight® 594	Abcam	Cat# ab96885
Rabbit monoclonal anti-AKT	Proteintech	Cat#60203-2-Ig
Rabbit monoclonal anti-mTOR	Proteintech	Cat#66888-1-Ig

Supplementary Table 4. Oligonucleotides sequences in this study.

The sequences of METTL1 shRNA	
No.	**sequence (**5’ - 3’**)**
shMETTL1-1	AAATGAGTGCACATCCAGTCG
shMETTL1-2	TTTCTTATCCTTTGGGTCATC
shWDR4-1	AAGAGGCTGTCATCATCACTG
ShWDR4-2	TCTAACAGCATAGACAGGTGC
The sequences of siRNA	
No.	**sequence (**5’ - 3’**)**
METTL1-1	GATGACCCAAAGGATAAGAAA
METTL1-2	GGATGTGCACTCATTTCGA
ULK1-1	CCTTCGCGGTGGTCTTCAAdTdT
ULK1-2	CGCGGTACCTCCAGAGCAAdTdT
Probe sequences of tRNAs and U6 snRNA	
No.	**sequence (**5’ - 3’**)**
tRNA-Lys-CTT	AACGTGGGGCTCGAACCCAC
tRNA-Val-AAC	TGTTTCCGCCCGGTTTCGAA
tRNA-Thr-TGT	CTAACCCCTGAGCTATGGAG
U6 snRNA	TGGAACGCTTCACGAATTTG
Primers used for the qRT-PCR assay	
No.	**sequence (**5’ - 3’**)**
hGAPDH-F	GTCTCCTCTGACTTCAACAGCG
hGAPDH-R	ACCACCCTGTTGCTGTAGCCAA
hβ-ACTIN-F	CACCATTGGCAATGAGCGGTTC
hβ-ACTIN-R	AGGTCTTTGCGGATGTCCACGT
hmTOR-F	AGCATCGGATGCTTAGGAGTGG
hmTOR-R	CAGCCAGTCATCTTTGGAGACC
hRPTOR-F	GATCGTCAACAGCTATCACACGG
hRPTOR-R	CGAGTCGAAGTTCTGCCAGATC
hMETTL1-F	GGCTTCCAGAACATCGCCTGT
hMETTL1-R	TGTCCGCTTGAAATGTGGGTCG
hWDR4-F	CGTCTACTCCTTTTCGGTGCTG
hWDR4-R	GCAGTGAGGATGAAGCGGTCAT
hAKT1-F	TGGACTACCTGCACTCGGAGAA
hAKT1-R	GTGCCGCAAAAGGTCTTCATGG
hPIK3C2A-F	CTTACTCATTGCTTCACCAGTGG
hPIK3C2A-R	GCCTCAATCCAGGTCACAGCTA
hPIK3CA-F	GAAGCACCTGAATAGGCAAGTCG
hPIK3CA-R	GAGCATCCATGAAATCTGGTCGC

hPIK3CB-F	GGTAATCGGAGGATAGGGCAGT
hPIK3CB-R	CGGCAGTATGCTTCAAGGATGAC
mGapdh-F	CATCACTGCCACCCAGAAGACTG
mGapdh-R	ATGCCAGTGAGCTTCCCGTTCAG
mRaptor-F	CTTCCTATCCGTCTTGGCAGAC
mRaptor-R	CTCCAGACAGATGGCAATCAGG
mMettl1-F	GTGGAGTTTGCAGACATAGGCTG
mMettl1-R	GCACATAGTCCGACACCTTCAC
Firefy-Luc-F	GGTACTGTTGGTAAAGCCAC
Firefy-Luc-R	CTCTTCATAGCCTTATGCAG
Renilla-Luc-F	CAATGGGCAGGTGTCCACTC
Renilla-Luc-R	GTTCTGGATCATAAACTTTC
Primers for floxed Mettl1 knockdown/knockin allele genotyping	
No.	**Sequence (**5’ - 3’**)**
Keratin14-CreER-1	ACTGGGATCTTCGAACTCTTTGGA C
Keratin14-CreER-2	GATGTTGGG GCACTGCTCATTCACC
Keratin14-CreER-3	CCATCTGCCACCAGCCAG
Keratin14-CreER-4	TCGCCATCTTCCAGCAGG
METTL1-cKO-F	ATACACACTCCT GGCCACTCC TTGT
METTL1-cKO-R	CCCTGGCTT CTA GGGTGTGAA TCAG
METTL1-cKI-WT-F	AGTCGCTCTGAGTTGTTATCAG
METTL1-cKI-WT-R	TGA GCATGTCTTTAATCTACCTCGATG
METTL1-cKI-MUT-F	AGTCGCTCTGAGTTGTTATCAG
METTL1-cKI-MUT-R	GTCAATGGAAAGTCCCTATTGGCGT